MucosalImmunology

www.nature.com/mi

ARTICLE

MUC4 is overexpressed in idiopathic pulmonary fibrosis and collaborates with transforming growth factor β inducing fibrotic responses

Javier Milara[1,2,3,4], Beatriz Ballester[4], M. J. Safont[5], Enrique Artigues[6], Juan Escrivá[7], Esteban Morcillo[1,3,4] and Julio Cortijo[3,4,8]

Several mucins are implicated in idiopathic pulmonary fibrosis (IPF); however, there is no evidence regarding the role of MUC4 in the development of IPF. Here we demonstrated that MUC4 was overexpressed in IPF patients ($n = 22$) compared with healthy subjects ($n = 21$) and located in pulmonary arteries, bronchial epithelial cells, fibroblasts, and hyperplastic alveolar type II cells. Decreased expression of MUC4 using siRNA–MUC4 inhibited the mesenchymal/myofibroblast transformations of alveolar type II A549 cells and lung fibroblasts, as well as cell senescence and fibroblast proliferation induced by TGF-β1. The induction of the overexpression of MUC4 increased the effects of TGF-β1 on mesenchymal/myofibroblast transformations and cell senescence. MUC4 overexpression and siRNA–MUC4 gene silencing increased or decreased, respectively, the phosphorylation of TGFβRI and SMAD3, contributing to smad-binding element activation. Immunoprecipitation analysis and confocal immunofluorescence showed the formation of a protein complex between MUC4β/p-TGFβRI and p-SMAD3 in the cell membrane after TGF-β1 stimulation and in lung tissue from IPF patients. Bleomycin-induced lung fibrosis was reduced in mice transiently transfected with siRNA–MUC4. This study shows that MUC4 expression is enhanced in IPF and promotes fibrotic processes in collaboration with TGF-β1 canonical pathway that could be an attractive druggable target for human IPF.

Mucosal Immunology (2021) 14:377–388; https://doi.org/10.1038/s41385-020-00343-w

INTRODUCTION

Idiopathic pulmonary fibrosis (IPF) is a chronic, progressive, and fatal form of fibrotic interstitial lung disease of unknown etiology, characterized by epithelial injury, chronic activation of invasive fibroblasts, and myofibroblast formation that deposits and remodels the extracellular matrix (ECM).[1] The origins of the invasive lung myofibroblasts, and the activation thereof, are not well known, but probably include activation of lung-resident fibroblasts and alveolar type II (ATII) epithelial-to-mesenchymal/myofibroblast transition (EMT).[2] Apoptosis-resistant senescence of alveolar epithelial cells and fibroblasts appears to be a central phenotype that promotes lung fibrosis through the increased production of a broad range of growth factors, cytokines, chemokines, and matrix metalloproteinases.[3] Although recent small-molecule drugs such as nintedanib[4] and pirfenidone[5] have been approved for the treatment of IPF, they have limited efficacy and notable toxicities.[6] Therefore, IPF remains a progressive disease and an unmet clinical need that requires new approaches and molecular targets.

Several lines of evidence link mucins to IPF disease, suggesting that they are key effectors of the disease.[7] Secreted MUC5B[8] and MUC5AC[9] gene variants have been associated with IPF; however, the role of transmembrane mucins in IPF is less known. MUC4 is a transmembrane mucin that has been observed overexpressed in lung tissue[7] and pulmonary arteries[10] from IPF patients, whose function in IPF is unknown.

MUC4 mucin consists of a large extracellular alpha subunit (MUC4α) that is heavily glycosylated and a beta subunit (MUC4β) that is anchored in the cell membrane and extends into the cytosol. The overexpression of MUC4α confers the anti-adhesive properties to the cell, allowing for cell–cell and cell–matrix detachment in normal as well as cancerous cells, increasing migration and invasive cell properties.[7,11] MUC4α is cleaved by nonenzymatic process releasing MUC4α chain to the extracellular space, which can be detected as a biomarker of different malignancies.[12] MUC4β subunit is rich in N-glycosylation sites and contains up to three extracellular epidermal growth factor (EGF)-like domains, a hydrophobic transmembrane region, and a 22-amino-acid cytoplasmic tail with two serine and one threonine potential phosphorylation sites. In contrast to MUC4α, MUC4β chain is considered an oncogene that modulates and activates different cellular signals and cellular phenotypic changes related with cellular proliferation, migration, and invasion.[7]

MUC4β serves as an intramembrane ligand for ErbB2 receptor via one of its EGF-like domains.[13] Enhanced stabilization of ErbB2 through MUC4β interaction activates the extracellular signal-regulated kinase (ERK) 1/2 MAPK, JNK, and STAT-1 pathways that

[1]Department of Pharmacology, Faculty of Medicine, University Jaume I, Castellón, Spain; [2]Pharmacy Unit, General University Hospital, Valencia, Spain; [3]CIBERES, Health Institute Carlos III, Valencia, Spain; [4]Department of Pharmacology, Faculty of Medicine, University of Valencia, Valencia, Spain; [5]Oncology department, University General Hospital Consortium, Valencia, Spain; [6]Surgery Unit, University General Hospital Consortium, Valencia, Spain; [7]Thoracic Surgery Unit, University and Polytechnic Hospital La Fe, Valencia, Spain and [8]Research and teaching Unit, University General Hospital Consortium, Valencia, Spain
Correspondence: Javier Milara (xmilara@hotmail.com) or Beatriz Ballester (beaballester7@gmail.com)
These authors contributed equally: Javier Milara, Beatriz Ballester

Received: 31 October 2019 Revised: 25 July 2020 Accepted: 18 August 2020
Published online: 4 September 2020

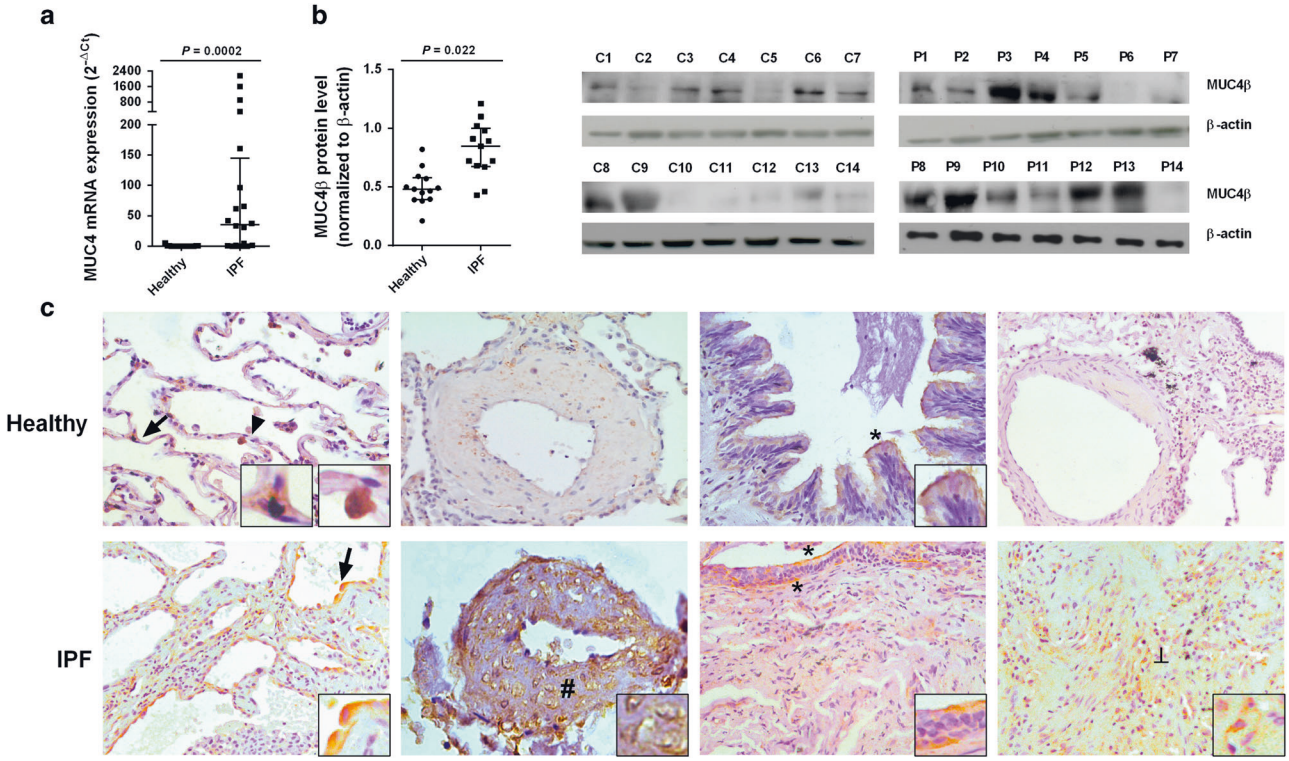

Fig. 1 MUC4 is overexpressed in lung tissue from idiopathic pulmonary fibrosis (IPF) patients. Lung tissue was obtained from healthy controls ($n = 21$) and IPF patients ($n = 22$). **a** MUC4 mRNA expression was analyzed by real-time polymerase chain reaction (PCR). **b** MUC4β protein expression levels were analyzed by western blotting ($n = 14$). **c** Immunohistochemistry of MUC4β. Scale bar: 100 μm. ATII cells (arrows), bronchial epithelium (*), alveolar macrophages (arrowhead), the innermost layer of the artery (#) and fibroblasts (⊥) show positivity for MUC4β immunostaining. Data are shown as the ratio compared to β-actin for protein expression and $2^{-\Delta Ct}$ for mRNA levels. Data are presented as a scatter dot plot with median and interquartile ranges. *P* values are based on the Mann–Whitney test.

promote cell proliferation and migration in vitro and enhance tumorigenicity and metastasis in vivo.[14] MUC4β induces lysosomal degradation of E-cadherin through downregulation of pFAK and pSrc pathway, increasing nuclear accumulation of β-catenin and activation of Wnt/β-catenin signaling pathway implicated in cell proliferation, metastasis, and angiogenesis.[15] The EMT process is also activated by the overexpression of MUC4β that increases mesenchymal/myofibroblast factors such as TWIST, ZEB1, SNAIL, N-cadherin, and vimentin, and decreases epithelial markers such as cytokeratin-18, E-cadherin, and occluding.[16,17] However, although MUC4β cell actions have been associated with the ErbB2 interaction, MUC4β can activate cellular processes independently of ErbB2, suggesting other unknown partners at the membrane via its different modular domains.[18]

Transforming growth factor-β (TGFβ) family proteins are considered the principal profibrotic cytokines and play a prominent role in lung fibrosis.[19] However, direct or indirect targeting of TGFβ activation has major side effects,[20,21] due to the pleiotropic roles of TGFβ family members. Therefore, the indirect modulation of TGFβ signal might be an alternative IPF therapy. In this work, we analyzed the expression and distribution of MUC4β in IPF, as well as the possible interaction of MUC4β with TGFβ signaling, which may represent a new role of MUC4 as a druggable target in IPF.

RESULTS

MUC4β is overexpressed in the lungs of IPF patients

MUC4 transcript ($n = 22$) and MUC4β protein ($n = 14$) expression levels were elevated in lung tissue from IPF patients compared to healthy controls (Fig. 1). Immunohistochemistry of control lung sections showed weak MUC4β expression that was mainly localized in ATII cells (arrows), surface of the bronchial epithelium (*) (mainly ciliated cells (Supplementary Fig. 1)), and alveolar macrophages (arrowhead) (Fig. 1c). In contrast, in IPF lung tissue, MUC4β was elevated in hyperplastic ATII cells (arrows), surface and basal bronchial epithelial cells (*), the innermost layer of the artery (#), and fibroblasts (⊥) (Fig. 1c), and was mainly localized in the membrane/cytoplasm. According to the regional differences based on the lung fibrotic extension within the explanted lungs, MUC4β expression also changed along the area sampled. In this context, MUC4β staining was increased in the cells experiencing a higher degree of fibrotic remodeling (Fig. 1c). These results are further supported by the absence of background staining after using the nonimmune IgG isotype in fibrotic lung tissue sections (Supplementary Fig. 2).

TGFβ1 collaborates with MUC4β to induce the ATII to mesenchymal and fibroblast-to-myofibroblast transitions

In A549 cells transiently transfected with siRNA–MUC4, TGFβ1 did not induce the ATII to mesenchymal transition, reducing the enhanced expression of αSMA, collagen type I, SLUG, and SNAIL, and elevating the expression of E-cadherin (Fig. 2). Similar results were observed in primary lung fibroblasts from IPF and healthy control subjects (Fig. 3b–i), as well as in the MRC5 lung fibroblast cell line (Fig. 4). In primary fibroblasts and MRC5 cells transiently transfected with siRNA–MUC4, TGFβ1 did not induce the fibroblast-to-myofibroblast transition, attenuating the increase in myofibroblast markers αSMA, collagen type I, SLUG, and SNAIL expression (Figs. 3b–i and 4). MUC4 expression was increased in primary fibroblasts from IPF patients (Fig. 3a) and after 72 h of TGFβ1 exposure in MRC5 cells (Fig. 4e).

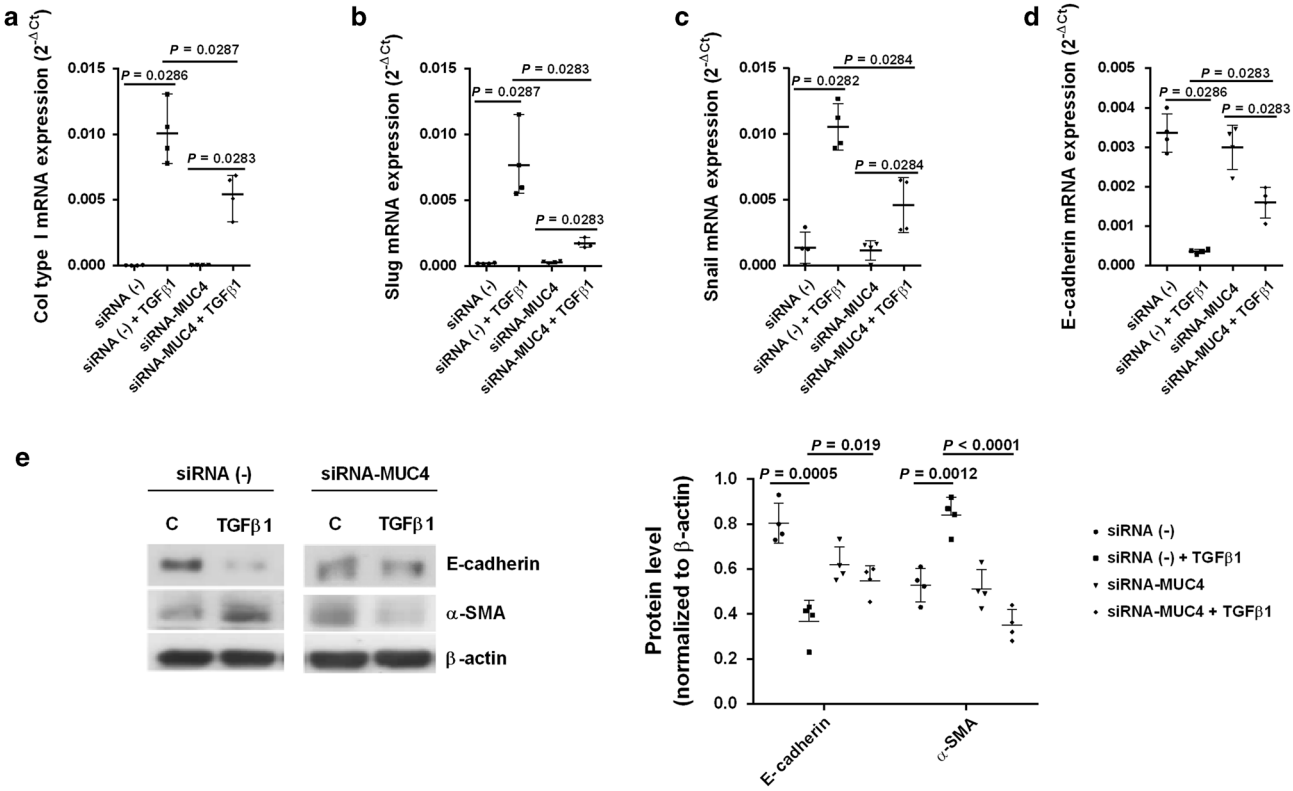

Fig. 2 TGF-β1 and MUC4β collaborate to induce the alveolar epithelial-to-mesenchymal transition. a–e The A549 cell line transfected with control siRNA(−) or siRNA–MUC4 was stimulated for 72 h with 5 ng/ml TGF-β1 to measure (**e**) α-SMA and E-cadherin by western blotting, and (**a**–**d**) collagen type I, Slug, Snail, and E-cadherin expression by real-time PCR. Data are expressed relative to β-actin protein, and to $2^{-\Delta Ct}$ for mRNA levels. Data are presented as a scatter dot plot with means ± ranges of $n = 4$ independent experiments. *P* values are based on the Mann–Whitney test.

MUC4β mediates cell senescence, proliferation, and epithelial-to-mesenchymal transition induced by TGF-β1

TGF-β1 at a dose of 10 ng/ml increased cell proliferation after 48 h of stimulation in MRC5 fibroblasts (Fig. 5a). After 72 h of exposure, lung fibroblasts showed increased β-galactosidase activity, thus indicating a change from active proliferative to senescent fibroblasts (Fig. 5b). Proliferative and senescent fibroblast phenotypes were inhibited in siRNA–MUC4-transfected cells. In other experiments, we observed that TGF-β1 increased the β-galactosidase activity in A549 cells that was inhibited in siRNA–MUC4-transfected cells (Fig. 5c).

HEK293/Tet3G/TRE3G-MUC4 stable cell line was created with doxycycline-inducible MUC4 expression system and full-length MUC4-inducible plasmid CS-H2247-pTREG. Doxycycline at 1 nM, 10 nM, 100 nM, and 1 μM induced 2×-, 19×-, 42×-, and 100×-fold MUC4 increased expression, respectively, following 24 h of incubation as previously outlined.[22] HEK293/Tet3G/TRE3G-MUC4 stable cell line was incubated with or without doxycycline (1 μM) during 24 h followed by the stimulation with TGF-β1 during 48 h. MUC4 mRNA expression was increased by 1.8 ± 0.4-fold after TGF-β1 stimulation and 10.2 ± 0.1-fold in cells pretreated with doxycycline confirming the upregulation of MUC4 in the cell system (Fig. 6g). TGF-β1 increased the expression of the senescence markers p16 and p21 that were significantly upregulated in HEK293/Tet3G/TRE3G-MUC4 cells pretreated with doxycycline compared with nontreated cells (Fig. 5e, f). TGF-β1 increased the expression of myofibroblast markers collagen type I, Slug, Snail, and αSMA, and decreased the expression of the epithelial marker E-cadherin in HEK293/Tet3G/TRE3G-MUC4 cells that was significantly higher in the presence of doxycycline (Fig. 6a–d, h). The expression of the TGF-β1 receptors TGFβRI and TGFβRII was not affected by pretreatment with doxycycline or by stimulation with TGF-β1 (Fig. 6e, f).

MUC4β mediates the phosphorylation of TGFβRI and SMAD3 induced by TGF-β1

TGF-β1 induced the phosphorylation of TGFβRI that was enhanced in HEK293/Tet3G/TRE3G-MUC4 cells pretreated with doxycycline (Fig. 7a). In alveolar epithelial A549 and lung fibroblast MRC5 cells, TGF-β1 increased the phosphorylation of TGFβRI that was inhibited in cells transiently transfected with siRNA–MUC4 (Fig. 7b, c).

HEK293/Tet3G/TRE3G-MUC4 cells were pretreated with doxycycline during 24 h to induce the expression of MUC4, and stimulated with TGF-β1 for 30 min to promote the phosphorylation of TGFβRI. Total protein was extracted and immunoprecipitated with MUC4β followed by an immunoblot with the p-TGFβRI antibody or MUC4β immunoblot (Fig. 7d). TGF-β1 promoted the formation of MUC4β/p-TGFβRI protein complex that was increased in the presence of doxycycline (Fig. 7d). Similarly, alveolar epithelial A549 and lung fibroblast MRC5 cells stimulated with TGF-β1 promoted the formation of MUC4β/p-TGFβRI protein complex (Fig. 7e, f). The stimulation of A549 cells with TGF-β1 promoted the cell membrane co-localization of MUC4β/p-TGFβRI assayed by confocal immunofluorescence (Supplementary Fig. 3A). In contrast to healthy lung tissue, MUC4β and p-TGFβRI were co-localized in lung tissue from IPF patients (Supplementary Fig. 3B).

In other experiments, TGF-β1 induced the phosphorylation of SMAD3 in HEK293/Tet3G/TRE3G-MUC4 cells that was enhanced in the group pretreated with doxycycline (Fig. 8a). The phosphorylation of SMAD3 induced by TGF-β1 was inhibited in A549 and MRC5 cells transiently transfected with siRNA–MUC4 (Fig. 8b, c). TGF-β1 induced Smad-binding element (SBE) activation in A549

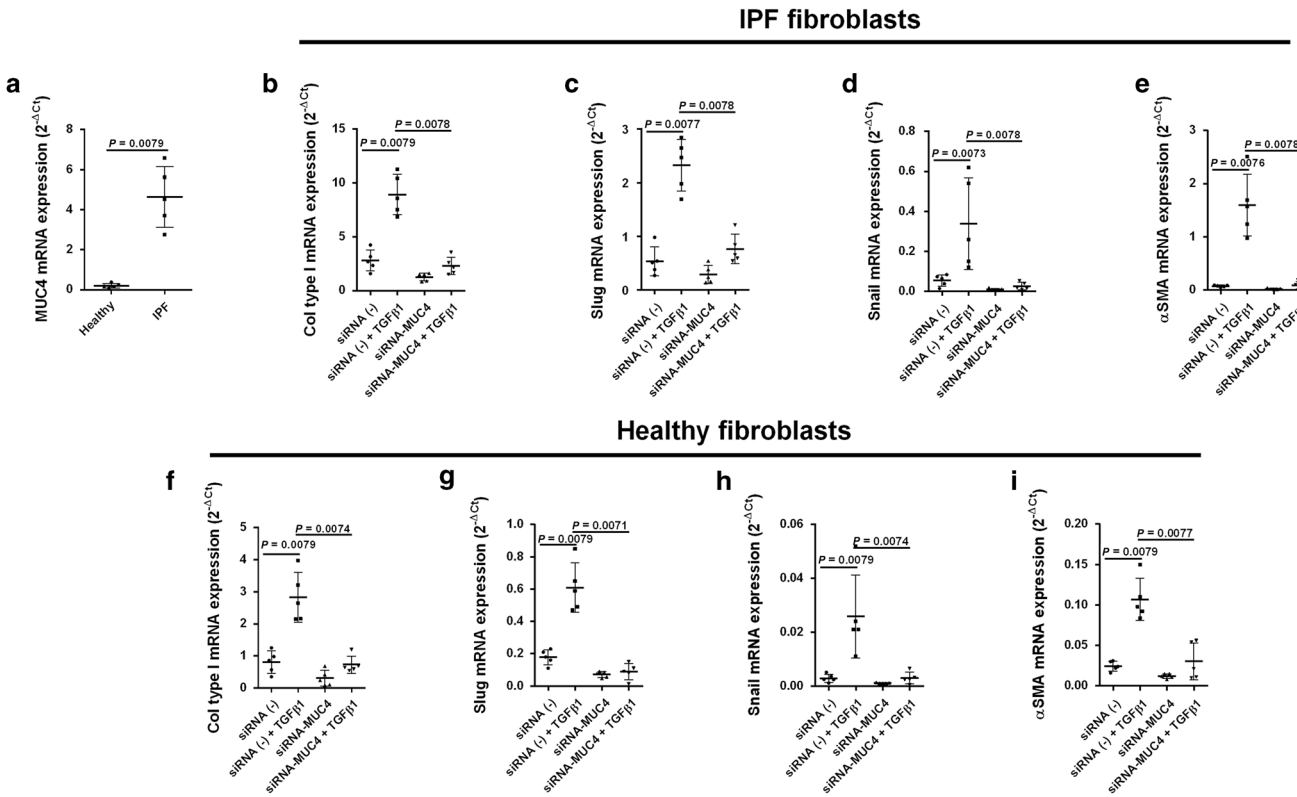

Fig. 3 TGF-β1 and MUC4β collaborate to induce the fibroblast-to-myofibroblast transition in primary fibroblasts. a MUC4 mRNA basal expression in primary fibroblasts from IPF patients and healthy control donors. **b**–**e** IPF lung fibroblasts and **f**–**i** healthy control lung fibroblasts transfected with control siRNA(−) or siRNA–MUC4 were stimulated for 72 h with 5 ng/ml TGF-β1 to measure collagen type I, Slug, Snail, and αSMA expression by real-time PCR. Data are expressed relative to β-actin protein, and to $2^{-\Delta Ct}$ for mRNA levels. Data are presented as a scatter dot plot with means ± ranges of $n = 5$ subjects. *P* values are based on the Mann–Whitney test.

cells, which was attenuated in cells transiently transfected with siRNA–MUC4, and increased in HEK293/Tet3G/TRE3G-MUC4 cells pretreated with doxycycline (Fig. 8d, e). In parallel experiments, immunoprecipitation analysis revealed a protein complex formation between MUC4β and p-SMAD3 after TGF-β1 stimulation in A549 and MRC5 cells (Fig. 8f, g). Confocal immunofluorescence also demonstrated co-localization between MUC4β and p-SMAD3 following TGF-β1 stimulation in the same way than in fibrotic lung tissue of IPF patients (Supplementary Fig. 4).

Lung fibrosis induced by bleomycin is reduced in MUC4-KO mice Intratracheal (IT) bleomycin administration induced robust lung fibrosis that increased the mortality of mice by ~40% after 14 days (Fig. 9a). Mortality was improved in MUC4-KO mice to ~15% (Fig. 9a), while wild-type (WT) control and MUC4-KO control mice showed 100% survival (overlapping red and blue lines). Bleomycin-treated WT animals showed increased Penh values; these were significantly lower in the MUC4-KO bleomycin group (Fig. 9b), suggesting improvement of lung function.

The IT bleomycin administration in WT mice produced greater numbers of inflammatory cells in BALF than seen in MUC4-KO mice (Fig. 8c, d). By contrast, WT and MUC4-KO control mice showed similar levels of BALF inflammatory cells (Fig. 9c, d). Furthermore, WT-bleomycin-treated mice showed larger lung fibrotic extension and higher collagen deposition than MUC4-KO-bleomycin-treated mice (Fig. 9e).

The mRNA gene and protein expression of recognized fibrotic markers such as collagen type I, TGF-β1, CTGF, IL-6, and IL-13, the fibrotic mucins MUC5B and MUC4, the oxidative fibrotic markers NOX4 and NRF2, and senescence mediator p21 were induced by bleomycin in lung tissue from WT mice, while MUC4-KO animals showed minimal elevation (Fig. 10 and Supplementary Fig. 5). The activation of downstream signals of TGF-β1, such as phosphorylated TGFβRI, p-Smad3, and p-Erk1/2, as well as the activation of β-catenin, were increased in bleomycin-treated WT mice, while MUC1-KO mice showed levels similar to those in untreated mice (Supplementary Fig. 5).

Immunofluorescence confocal micrographs of mouse lung sections showed co-localization of MUC4β/p-TGFβRI and MUC4β/p-SMAD3 in lung tissue from WT-bleomycin-treated mice but not in MUC4-KO-bleomycin-treated mice (Supplementary Fig. 6).

DISCUSSION

The present work shows first evidence of the MUC4β expression and distribution in lungs from IPF patients, as well as the interaction of MUC4β chain with the TGF-β1 canonical signal pathway promoting fibrotic cellular effects.

Recent evidences have demonstrated that MUC4 is overexpressed and participates in invasive cellular processes involved in different malignances, including tumors of the lung, breast, pancreas, colon, and ovary.[23] However, currently, there is a lack of evidence about the role of MUC4 in fibroproliferative disorders such as pulmonary fibrosis. It has been reported that almost 50% of end-stage IPF patients are awaiting lung-transplant display pulmonary hypertension (PH).[24] In this context, recent whole-genome expression data from pulmonary arteries of IPF patients with PH showed a significant overexpression of MUC4 compared to pulmonary arteries from non-IPF patients without PH.[10] Although the later study was focused on pulmonary artery remodeling from IPF patients, the data suggest an overexpression

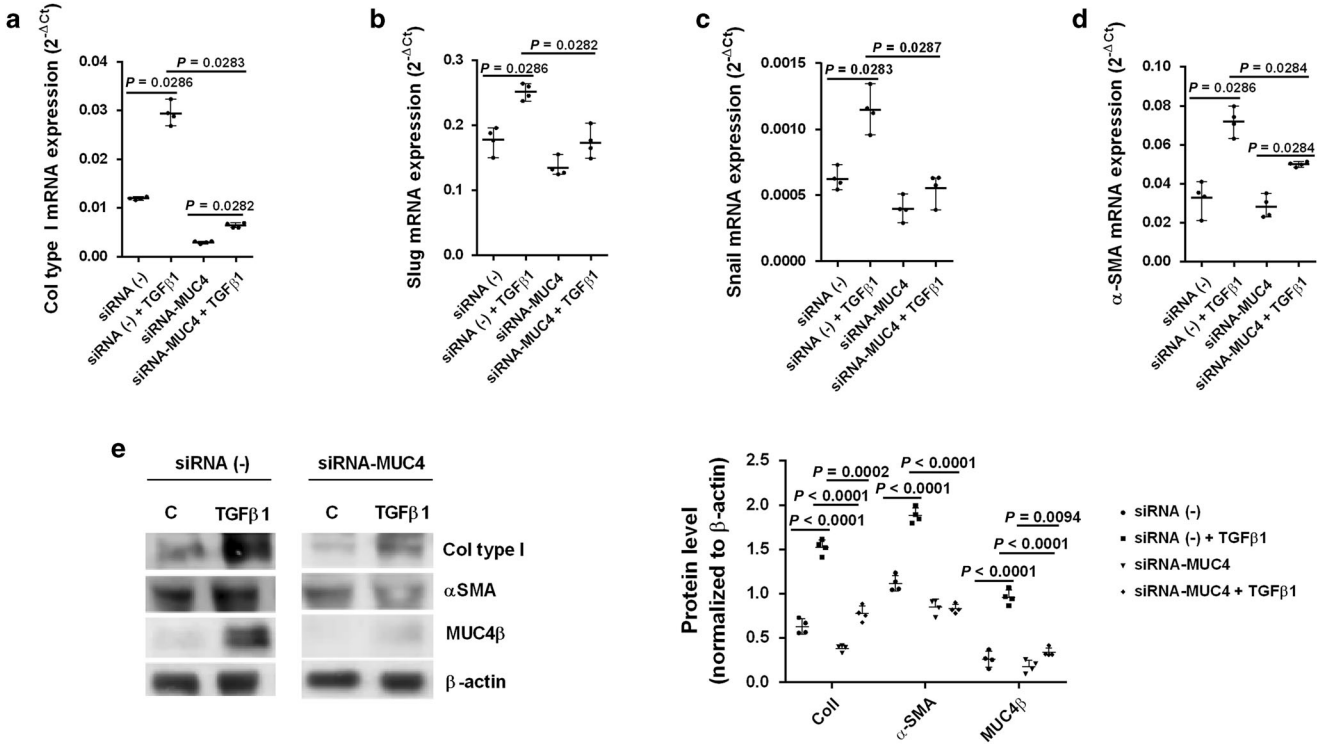

Fig. 4 TGF-β1 and MUC4β collaborate to induce the fibroblast-to-myofibroblast transition. a–**e** The MRC5 cell line transfected with control siRNA(−) or siRNA–MUC4 was stimulated for 72 h with 5 ng/ml TGF-β1 to measure (**a**) collagen type I, (**b**) Slug, (**c**) Snail and (**d**) αSMA expression by real-time PCR, and (**e**) collagen type I, α-SMA, and MUC4β by western blotting. Data are expressed relative to β-actin protein, and to $2^{-\Delta Ct}$ for mRNA levels. Data are presented as a scatter dot plot with means ± ranges of $n = 4$ independent experiments. *P* values are based on the Mann–Whitney test.

in lung fibrotic parenchyma. In this study, we have confirmed this hypothesis, showing that MUC4 is overexpressed in lung tissue of IPF patients compared with healthy donors, and that MUC4 expression was located in parenchyma, pulmonary arteries, and bronchial epithelium. Although the pulmonary artery pressure data from IPF patients included in this study were absent, we can presume some degree of PH due to the severity of lung function parameters. Therefore, we hypothesize that MUC4 expression levels might be a clinical driver of the degree of PH development in the IPF patients included in this study. In line with this, future studies should assess the clinical correlation between MUC4 expression and the degree of PH in IPF patients.

By this time, clinical correlation between MUC4 expression and lung function parameters has not been published yet. However, it has been previously published that under a hypoxic environment, MUC4 is upregulated in pancreatic tissue,[25] although no data are available in lung tissue. In this context, potential further studies are required to assess if MUC4 expression levels also positively correlate with the degree of PH in IPF patients.

MUC4 cellular distribution in IPF lung tissue was located in pathologic hyperplastic ATII cells, lung fibroblast from fibrotic foci, and apical and basal bronchial epithelial cells, indicating a possible role of MUC4 in IPF cellular processes. Previously to this work, higher expression levels of MUC4 in MUC5B+ cells were already registered in the IPF Cell Atlas (http://www.ipfcellatlas.com/). MUC5B has been largely reported as a proven lung fibrosis mediator.[8,26] Therefore, it supports the possible role of MUC4 in IPF. Indeed, perhaps, MUC5B/MUC4 dual pathway might be considered in IPF.

This study was limited to the expression and molecular role of MUC4 in IPF; however, MUC4 genotyping could be an attractive strategy to analyze the role of MUC4 in this disease. However, similarly to the previously identified *rs35705950* MUC5B polymorphism,[26] future studies focused on MUC4 genotyping might be an interesting approach to identify if there is some relevant polymorphism driving MUC4 expression in IPF patients.

MUC4 mucin is synthesized as a single polypeptide chain of ~930 kDa, generating two subunits after proteolytic cleavage at GDPH site, the extracellular mucin-type subunit MUC4α and a transmembrane subunit MUC4β.[7] The α subunits of MUC4 are responsible for its function as mucin, participating in epithelial cell defense, lubrication, and cell adherence, and the β subunit appears to contribute to cellular growth signaling and cell transformation.[27] Therefore, in this work, we focused on MUC4β subunit in both IPF tissue/cell distribution and cell function.

MUC4β signaling appears to be mediated by the extracellular region of the MUC4β subunit. The MUC4β extracellular region contains three EGF-like domains. It has been demonstrated that MUC4β and HER2 associate when the two proteins are co-expressed in the same cells.[28] Expression of MUC4β elevates HER2 tyrosine kinase phosphorylation,[29] thus activating MAPK pathway and β-catenin nuclear internalization.[15] While MUC4β/HER2 complex is associated with healthy epithelial repair after wound injury,[29] the aberrant MUC4β expression has been associated with cell proliferation, epithelial to mesenchymal transformation, and cancer metastasis.[30]

Aberrant EGFR signaling is associated with the early-stage pathogenesis of lung fibrosis; however, its overexpression and activation are restricted to HER1 rather than HER2.[31,32]

This fact oriented our investigation to the isolated effects of MUC4β since it has been reported that MUC4 elevates the survival of cell lines that lack either HER receptor expression or activation upon MUC4 expression.[33] These observations point to the existence of at least one other pathway through which MUC4 influences cellular effects.

TGF-β1 is a potent fibrotic growth factor that is increased and activated in IPF. However, the efforts to target TGFβ activation have

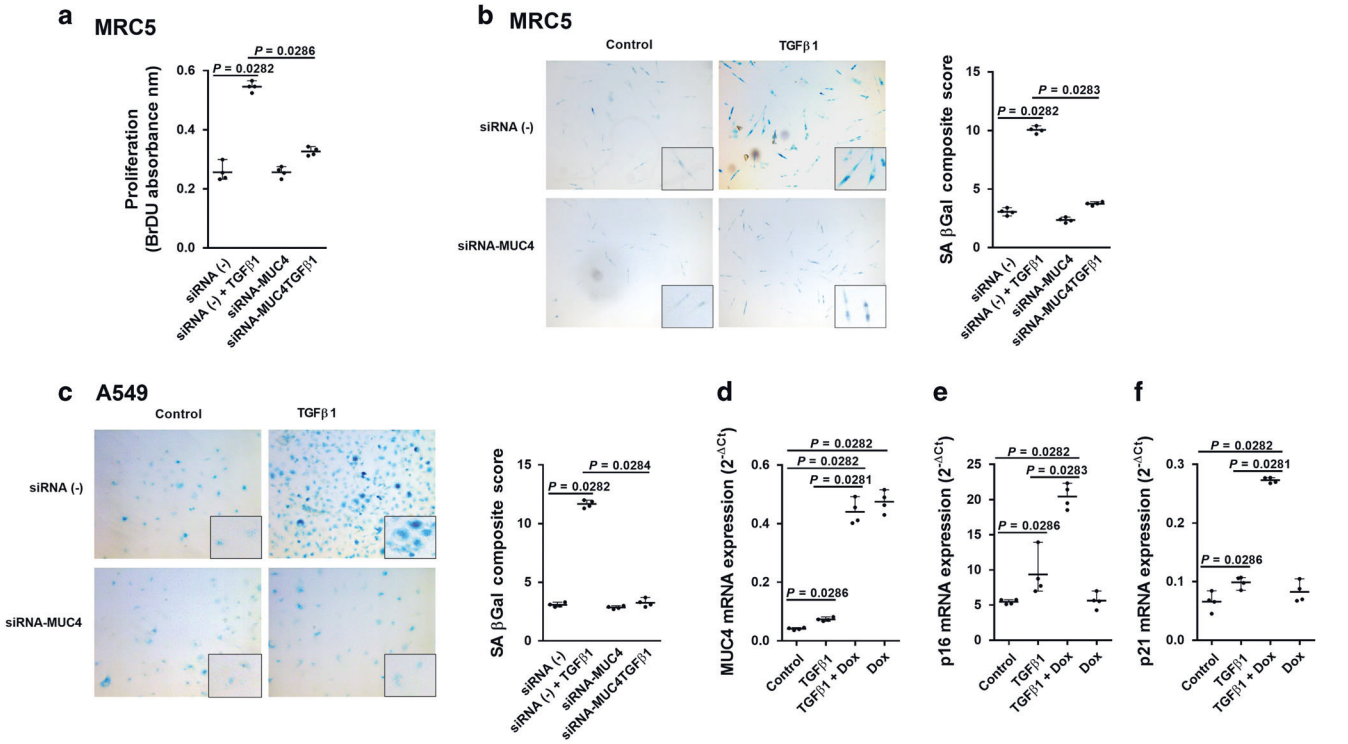

Fig. 5 MUC4 mediates TGF-β1-induced lung fibroblast proliferation and senescence of epithelial alveolar cells and fibroblasts. a TGF-β1 10 ng/ml was added in siRNA–MUC1 or siRNA(–) lung MRC5 fibroblasts during 48 h, and proliferation was evaluated by the BrdU assay. **b**, **c** Percentage of MRC5 fibroblasts or alveolar epithelial A549 cells expressing blue-staining β-galactosidase from the total number of siRNA–MUC1 or siRNA(–) cells after 72 h of TGF-β1 stimulation. **d**–**f** HEK293/Tet3G/TRE3G-MUC4 cells stimulated with doxycycline for 24 h to induce MUC4 expression followed by the stimulation with TGF-β1 10 ng/ml for 78 h. The expression of **d** MUC4, **e** p16, and **f** p21 was measured by real-time PCR. Data are presented as a scatter dot plot with means ± ranges of $n = 4$ independent experiments. *P* values are based on the Mann–Whitney test.

major side effects,[20,21] and clinical use has been disappointed. In this line, modulation of TGF-β1 pathway could be an alternative therapeutic strategy. In this work, we hypothesized that MUC4β could interact with the TGF-β1 pathway modulating lung fibrosis and key cellular processes involved in pulmonary fibrosis such as EMT, fibroblast-to-myofibroblast transition, cell senescence, and proliferation.[2,34] The effects of TGF-β1 on alveolar EMT, fibroblast-to-myofibroblast transition, cell senescence, and fibroblast proliferation were inhibited when the expression of MUC4 was repressed by siRNA–MUC4 cell transfection. On the contrary, the overexpression of MUC4 using inducible HEK293/Tet3G/TRE3G-MUC4 stable cell line increased the effects of TGF-β1 on myofibroblast transformation and cell senescence. Myofibroblasts are key cellular components of pulmonary fibrosis that share fibroblast cell characteristics, such as the ability to secrete the ECM, and smooth muscle cell fibers that allow myofibroblasts to contract and migrate to invade lung tissue.[35] The origin of myofibroblasts has been broadly discussed, and possibly mesenchymal transition from aberrant alveolar epithelial type II cells and transformation of resident fibroblasts to myofibroblasts can be present.[2] Thus, the role of MUC4β on cellular transformations seen in this work, together with the antiapoptotic/senescence and fibroblast-proliferative properties, could have translational value to IPF. The fact that we used A549, MRC5, and HEK293 cell lines to explore the role of MUC4β on the fibrotic effects of TGF-β1 could be interpreted as a limitation of this study, since the use of primary cells from IPF patients would have been more appropriate. However, the elevated cell number and the cell stability required to perform gene silencing and plasmid transfection assays justify the use of cell lines instead of primary cells. Nevertheless, at least primary fibroblasts have been used to assess MUC4 basal expression in fibroblasts from IPF vs. healthy lung tissue, as well as the influence of performing siRNA–MUC4 transfection on the TGF-β1-induced FMT process (Fig. 3). Although we have generated some evidence on the expression/function of MUC4β in different cell types relevant to IPF, we do not know whether these functions can be translated to other lung cell types such as basal bronchial epithelial cells, pulmonary artery endothelial cells, or pulmonary artery smooth muscle cells, which guarantees further future studies.

The next approximation was to investigate whether MUC4β modulates TGF-β1 signaling. TGFβ exerts its action by binding to and inducing formation of cell surface receptor complexes consisting of type I (TGFβRI) and type II (TGFβRII) serine–threonine kinase receptors. Upon ligand binding, TGFβRII phosphorylates and activates TGFβRI. The resulting heteromeric complex facilitates the phosphorylation and subsequent activation of the intracellular SMAD canonical pathway.[36] In the present work, HEK293 cells overexpressing MUC4 showed an increased phosphorylation of TGFβRI and SMAD3 in response to the ligand TGF-β1. In the same way, alveolar epithelial cells and lung fibroblasts transiently transfected with siRNA–MUC4 with reduced expression of MUC4 showed an inhibition of phosphorylation of TGFβRI and SMAD3 in response to TGF-β1. These results indicate that some kind of interaction may be present between TGF-β1 system and MUC4β. Immunoprecipitation experiments showed that TGF-β1 induces a protein complex formation between MUC4β/p-TGFβRI/p-SMAD3 that increased when MUC4β was overexpressed. In the same way, MUC4β/p-TGFβRI and MUC4β/p-SMAD3 complexes induced by TGF-β1 were co-localized in plasmatic membrane of alveolar epithelial cells and also in cells from IPF lung tissue and in lung tissue from bleomycin-treated animals. The formation of the protein complexes activated the Smad-binding element that regulates the gene expression of SMAD3 profibrotic-dependent genes (Supplementary Fig. 7). The profibrotic role of MUC4 was confirmed in vivo using a

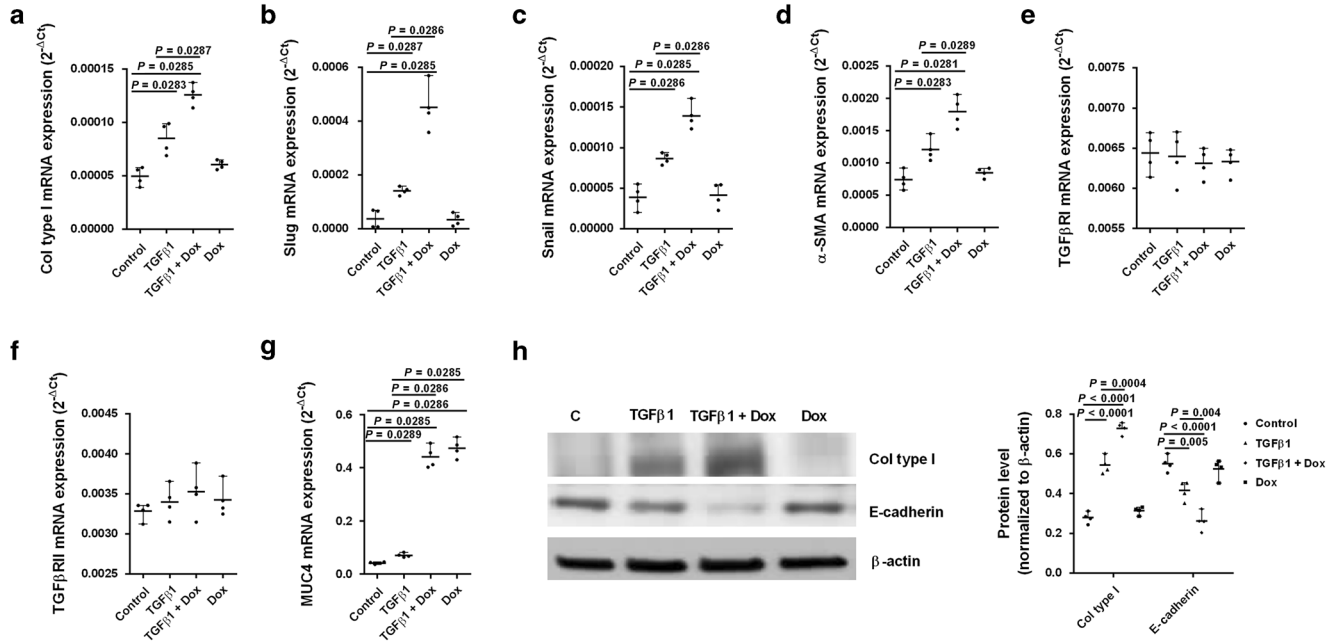

Fig. 6 The overexpression of MUC4 enhances the effects of TGF-β1 on epithelial-to-mesenchymal transition in transfected HEK293 cells. **a**–**h** HEK293/Tet3G/TRE3G-MUC4 cells stimulated with doxycycline for 24 h to induce MUC4 expression were stimulated with TGF-β1 10 ng/ml for 78 h. The expression of **a** collagen type I, **b** Slug, **c** Snail, **d** αSMA, **e** E-cadherin, **f** TGFβRI, and **g** TGFβRII was measured by real-time PCR, and the expression of **h** collagen type I and E-cadherin by western blot. Data are expressed relative to β-actin protein, and to $2^{-\Delta Ct}$ for mRNA levels. Data are presented as a scatter dot plot with means ± ranges of $n = 4$ independent experiments. *P* values are based on the Mann–Whitney test.

pulmonary fibrosis animal model induced by intratracheal bleomycin instillation.[37] In vivo gene silencing of MUC4 attenuates lung fibrosis induced by bleomycin in mice, improving survival, and reducing the profibrotic gene- and protein expression profile of proven lung fibrosis mediators such as collagen type I,[38] CTGF,[39] TGFβ1,[38] IL-13,[40] MUC5B,[8] NOX4,[41] Nrf2,[41] IL-13,[42] IL-6,[43] and p21.[44] These results confirmed those observed in vitro and can explain the effects of overexpression of MUC4 in lung tissue from IPF patients. Nevertheless, as the bleomycin pulmonary fibrosis animal model is initially characterized by a peak of inflammation prior to the fibrotic phase, and we have silenced MUC4 from the start of the bleomycin model, it might not be claimed that the in vivo silencing of MUC4 only affects the fibrotic phase, which represents a limitation of this study. SiRNA–MUC4 administration at day 7 of the experimental procedure would be more appropriate.

In summary, the data presented in this work show for the first time the overexpression and pathologic distribution of MUC4β in lung tissue from IPF patients. The overexpression of MUC4β cooperates with the phosphorylation of TGFβRI and SMAD3 signaling promoting fibrotic cellular disorders that could be targeted as future therapy in IPF.

METHODS

IPF lung tissue was obtained from patients undergoing surgery for organ transplantation ($n = 22$). Lung explant control samples were obtained from the organ-transplant program of the University General Hospital of Valencia, Spain ($n = 21$).

IPF was diagnosed according to the American Thoracic Society/European Respiratory Society consensus criteria.[45] The protocol was approved by the local research and ethics committee of the University General Consortium Hospital of Valencia (CEI CHGUV/052016). Informed written consent was obtained from all participants. Clinical data are provided in supplementary table S1. Detailed descriptions of additional materials and methods are provided in the online data supplement.

Isolation and culture of human lung fibroblast

Primary human lung fibroblasts were obtained from lung parenchyma of macroscopically fibrotic affected areas of IPF patients and from that of healthy control patients, and cultured as previously outlined.[46]

Culture of alveolar A549 epithelial cells and lung MRC5 fibroblast

The bronchoalveolar A549 cell line has been used to model epithelial ATII behavior. The A549 cell line and normal lung fibroblast MRC5 were purchased from American Type Culture Collection (Rockville, MD, USA) and cultured as previously outlined.[47]

Western blotting, immunoprecipitation, histological, immunohistochemical, and immunofluorescence studies

Western blotting analysis was used to detect changes in human and mice lung tissues, and A549 and MRC5 cell protein expression as previously outlined.[47] Antibodies used in this work are described in online supplementary data. Lung histology was conducted as previously reported.[48] For the immunoprecipitation analysis, equal amounts of protein (200 µg) from total protein extracts were incubated with 2 µg of p-Smad3, p-TGFβRI or anti-MUC4β antibodies, and the IgG isotype control, and precipitated with protein G on Sepharose 4B fast-flow beads (Sigma Aldrich, catalog no. P-3296).

For immunohistochemical analysis of human lungs, tissue was fixed and embedded in paraffin, cut into sections (4–6 µm), and incubated with MUC4β and CTGF antibodies for 24 h at 4 °C. A secondary anti-rabbit or anti-mouse antibody (1:100, Vector Laboratories, Burlingame, CA) with avidin–biotin complex/horseradish peroxidase was used for immunohistochemistry. The nonimmune IgG isotype control was used as negative control and became negative for all samples. MUC4β, p-Smad3, and p-TGFβRI in lung tissue, A549, and MRC5 cells were analyzed by immunofluorescence as previously outlined.[22] Details are provided in the online supplementary data.

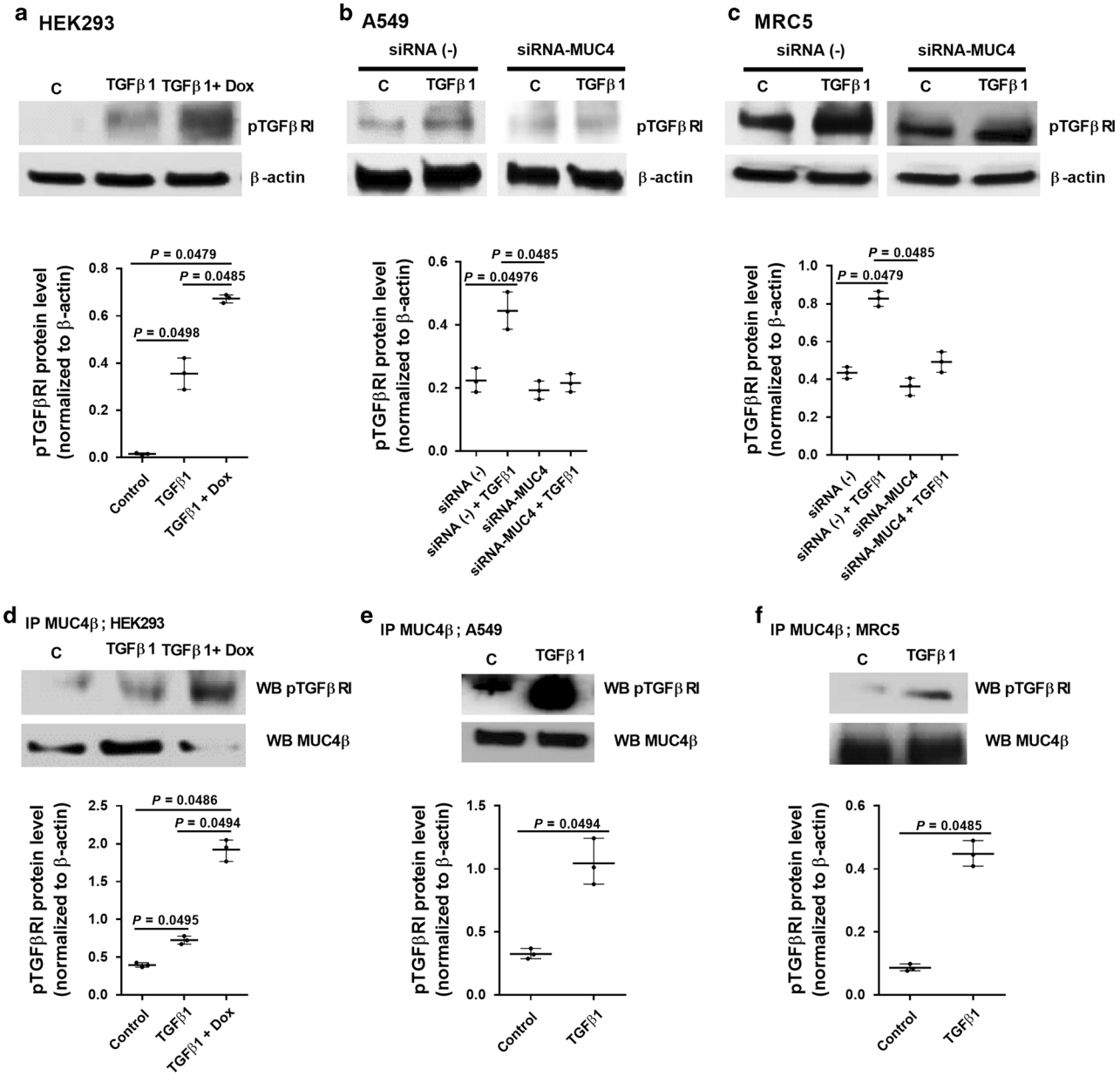

Fig. 7 MUC4 modulates the effect of TGF-β1 on TGFβRI phosphorylation. a HEK293/Tet3G/TRE3G-MUC4 cells were pretreated with doxycycline during 24 h to induce the expression of MUC4, and stimulated with TGF-β1 for 30 min to promote the phosphorylation of TGFβRI. **a** Protein expression of p-TGFβRI measured by western blot. **b** A549 and **c** MRC5 cell lines transfected with control siRNA(−) or siRNA–MUC4 were stimulated for 30 min with TGF-β1 10 ng/ml to measure p-TGFβRI by western blot. **d** HEK293/Tet3G/TRE3G-MUC4 cells pretreated or not with doxycycline and stimulated with TGF-β1 10 ng/ml during 30 min. **e**, **f** A549 and MRC5 cells transfected with control siRNA(−) or siRNA–MUC4 were stimulated for 30 min with TGF-β1 10 ng/ml. **d**–**f** Cells were immunoprecipitated using MUC4β antibody and probed against p-TGFβRI and MUC4β by western blot. Data are expressed relative to β-actin or MUC4β protein. Data are presented as a scatter dot plot with means ± ranges of $n = 3$ independent experiments. *P* values are based on the Mann–Whitney test.

Real-time RT-PCR and siRNA experiments

Total RNA was isolated using TriPure® Isolation Reagent (Roche, Indianapolis, USA). The integrity of the extracted RNA was confirmed with Bioanalyzer (Agilent, Palo Alto, CA, USA). Reverse transcription was performed in 300 ng of total RNA with a TaqMan reverse transcription reagent kit (Applied Biosystems, Perkin-Elmer Corporation, CA, USA). cDNA was amplified with specific primers and probes predesigned by Applied Biosystems and described in the online supplementary data.

Small-interfering RNA (siRNA), including the scrambled siRNA control, was purchased from Ambion (Huntingdon, Cambridge, UK, catalog no. 4390843). MUC4 gene-targeted siRNA (identification no. 144412) was designed by Ambion Co. The transfection reagent used was lipofectamine-2000 (Invitrogen, Paisley, UK, catalog no. 11668-027) at a final concentration of 2 μg/ml.

Cell proliferation and senescence

Fibroblast proliferation was measured by colorimetric immunoassay based on BrdU incorporation during DNA synthesis using a cell proliferation enzyme-linked immunosorbent assay BrdU kit (Roche, Mannheim, Germany) as previously outlined.[47] The senescence cell histochemical staining kit (Sigma Aldrich, catalog no. CS0030) based on a histochemical staining for

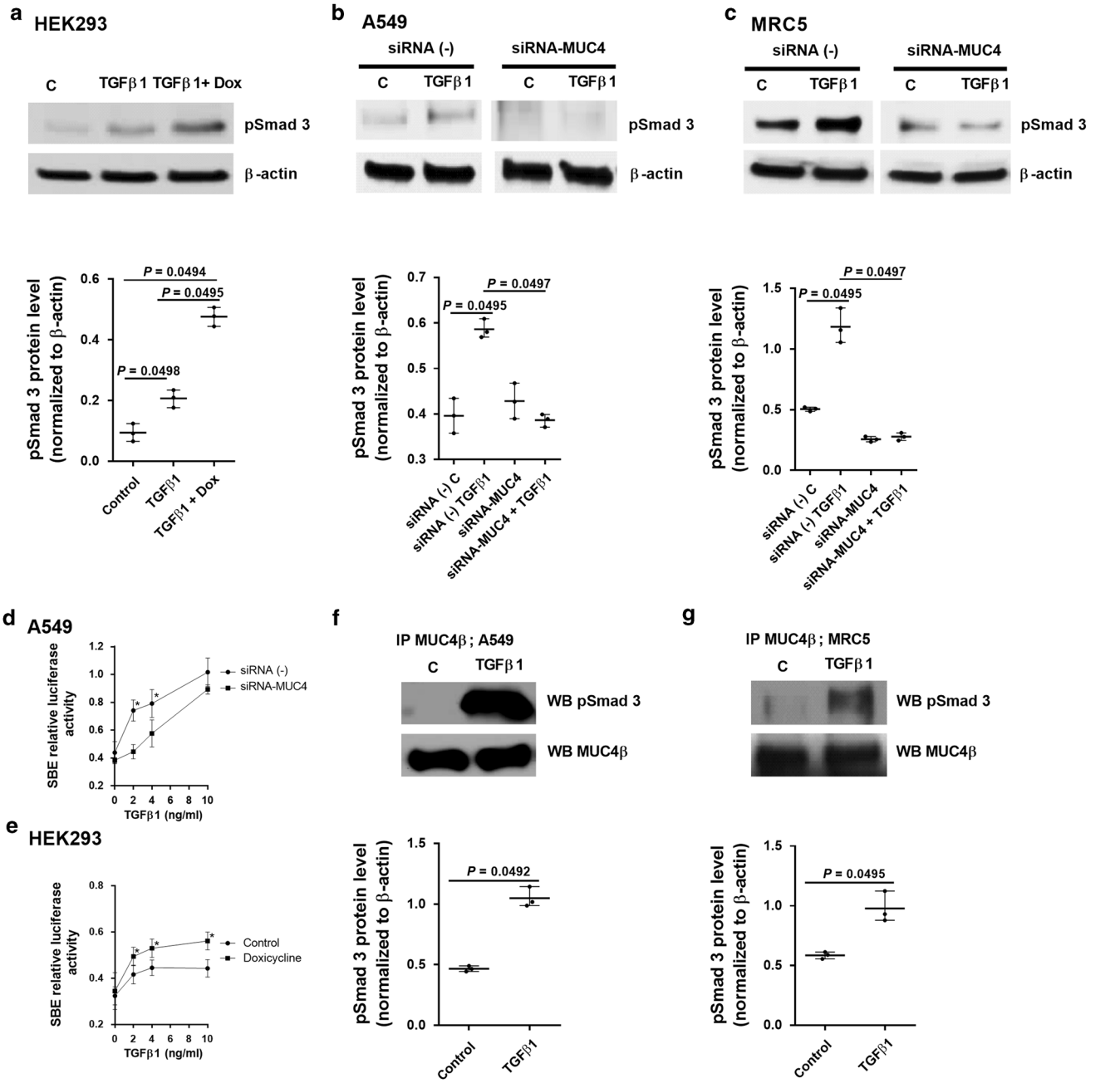

Fig. 8 MUC4 modulates the effect of TGF-β1 on SMAD3 phosphorylation. a HEK293/Tet3G/TRE3G-MUC4 cells were pretreated with doxycycline during 24 h to induce the expression of MUC4, and stimulated with TGF-β1 for 30 min to promote the phosphorylation of TGFβRI. **a** Protein expression of p-Smad3 measured by western blot. **b** A549 and **c** MRC5 cell lines transfected with control siRNA(−) or siRNA–MUC4 were stimulated for 30 min with TGF-β1 10 ng/ml to measure p-Smad3 by western blot. **d** Smad-binding element (SBE) measure following TGF-β1 stimulation in **d** A549 cells transfected with siRNA(−) or siRNA–MUC4 and in **e** HEK293/Tet3G/TRE3G-MUC4 cells pretreated with doxycycline. **f**, **g** Cells were immunoprecipitated using MUC4β antibody and probed against p-Smad3 and MUC4β by western blot. Data are expressed relative to β-actin or MUC4β protein. Data are presented as a scatter dot plot with means ± ranges of $n = 3$ independent experiments. *P* values are based on the Mann–Whitney test.

β-galactosidase activity was used. Details are provided in the online supplementary data.

Doxycycline-induced MUC4 expression in HEK293/Tet3G/TRE3G-MUC4 stable cell line

HEK293 cell line was acquired from the American Type Culture Collection and cultured in Dulbecco's Modified Eagle Medium (DMEM, Lonza, Madrid, Spain). The MUC4-inducible plasmid by doxycycline was constructed as Tet3G/TRE3G-MUC4 plasmid and transfected, creating a stable HEK293/Tet3G/TRE3G-MUC4 cell line as previously described.[22] Details are provided in online supplementary data.

SBE assay in siRNA-transfected cells

The SBE Reporter kit (Cat#: 60654, BPSBioscience) was used for monitoring the activity of TGFβ/SMAD signaling pathway in the

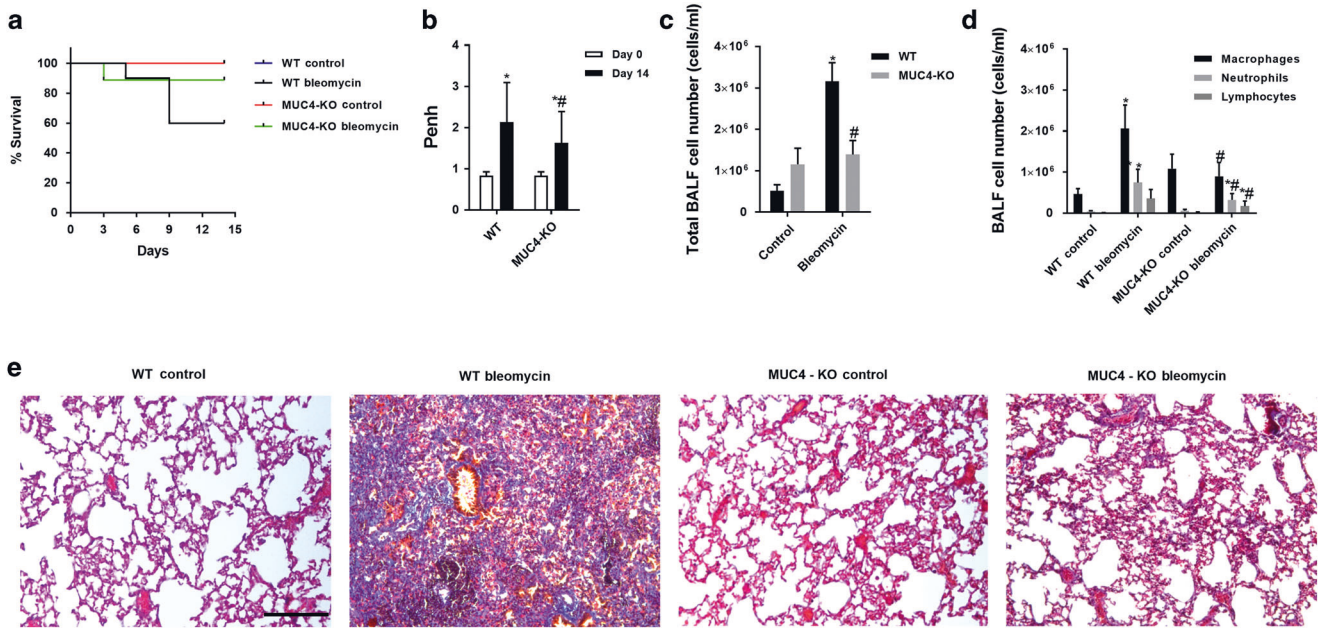

Fig. 9 MUC4 knockout (KO) improves survival and inhibits bleomycin-induced lung fibrosis. Wild-type (WT) siRNA(–) C57BL/6 mice and MUC1-KO siRNA–MUC4 C57BL/6 mice received a single intratracheal dose of bleomycin (1.5 U/kg) on day 1 ($n = 10$). **a** Kaplan–Meier survival analysis of mice treated with bleomycin for 14 days. **b** Pulmonary functions were evaluated as enhanced respiratory pause (Penh) on day 14 after bleomycin administration. Whole-body plethysmography was performed, and Penh was used as a noninvasive index of airway dysfunction. **c** Total and differential **d** bronchoalveolar lavage fluid (BALF) inflammatory cells. **e** Masson's trichrome staining of lung sections. The results are expressed as means ± SE (10 mice per group). Two-way ANOVA was followed by the post hoc Bonferroni test. $^{*}P < 0.05$ vs. control; $^{\#}P < 0.05$ vs. WT.

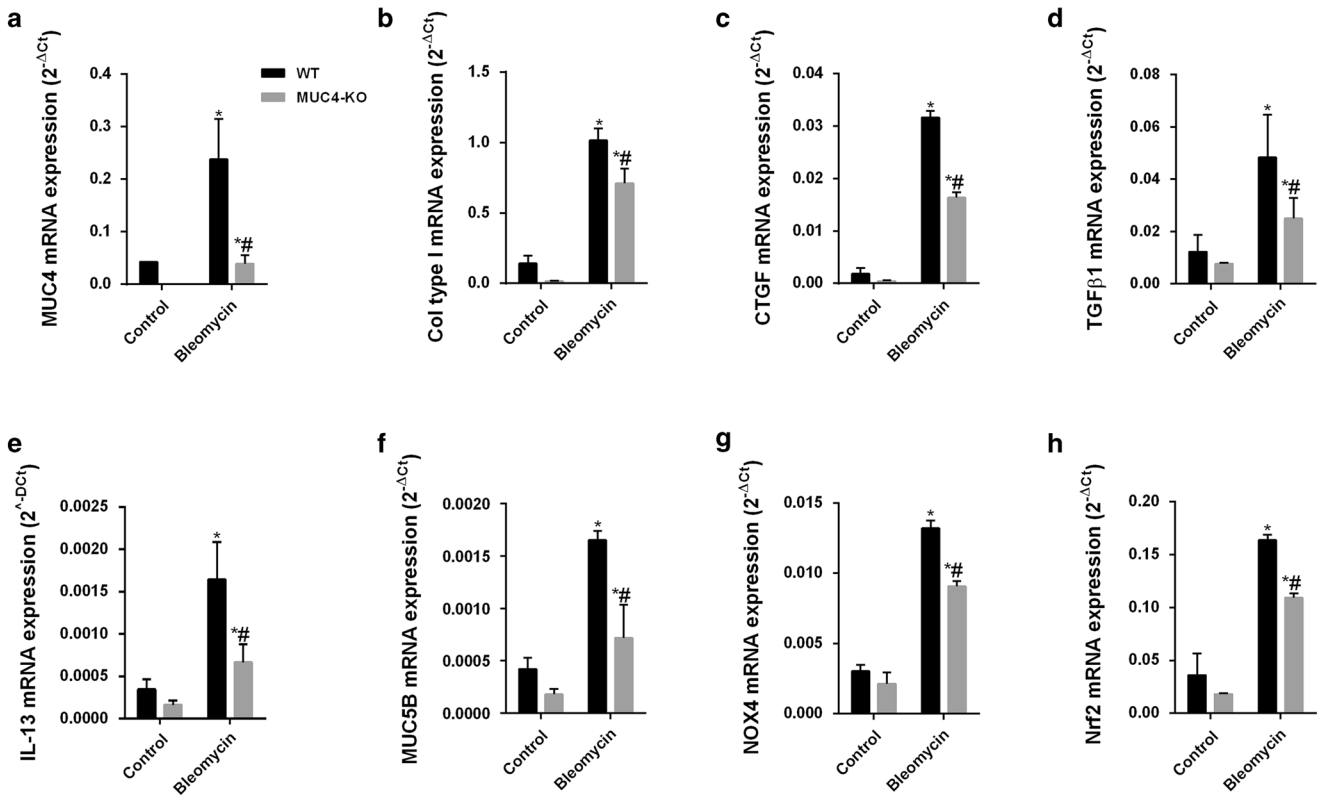

Fig. 10 MUC4 knockout (KO) inhibits the bleomycin-induced mRNA expression of molecular markers of lung fibrosis. Wild-type (WT) siRNA(–) C57BL/6 mice and MUC1-KO siRNA–MUC4 C57BL/6 mice received a single intratracheal dose of bleomycin (1.5 U/kg) on day 1 ($n = 10$). **a** Total RNA from lung tissue was analyzed by qPCR. **a** MUC4, **b** collagen type I, **c** CTGF, **d** TGF-β1, **e** IL-13, **f** MUC5B, **g** NOX4, and **h** Nrf2 were analyzed by qPCR. The results are expressed as means ± SE (10 mice per group). Two-way ANOVA was followed by the post hoc Bonferroni test. $^{*}P < 0.05$ vs. control; $^{\#}P < 0.05$ vs. WT.

cultured cells according to the manufacturer's instructions. Details are provided in online supplementary data.

Fibrosis animal model

Experimentation and handling were performed in accordance with the guidelines of the Committee of Animal Ethics and Well-being of the University of Valencia (Valencia, Spain, 2017/VSC/PEA/00061). The animal studies followed the ARRIVE guidelines.[49] Mice studies used pathogen-free male C57BL/6 of 12 weeks old (Harlan Iberica®, Barcelona, Spain). Transient MUC4-KO mice C57BL/6 animals were generated as follows: for in vivo RNAi studies, Muc4 siRNA (ID 257492, Ambion) or nontargeting control siRNA (Cat#: 4404021, Ambion) were reconstituted (5 µg/µl) in nuclease-free water and administered to the lungs to 12-week-old mice by intranasal and intravenous delivery. Intranasal delivery was at a dose of 50 µg per treatment in a total volume of 20 µl of PBS. Intravenous delivery was as siRNA/polyethylenimine linear (in vivo-jetPEI®, Polyplus-transfection S.A.) complexes. A dose of 40 µg of siRNA was diluted into 100 µl of 5% glucose, and a dose of 6.4 µl of polyethylenimine was diluted into 100 µl of 5% glucose. In both cases, 10% glucose stock solution was used. Diluted polyethylenimine was added to the diluted siRNA all at once, vortexed gently, and spun down. The mix was incubated for 15 min at room temperature and immediately delivered into the tail vein. Intranasal and intravenous delivery were repeated during 14 days every 72 h.

Bleomycin-induced lung fibrosis animal model was established as previously outlined.[37] Details are provided in online supplementary data.

Statistical analysis

Statistical analysis of the results was carried out by parametric (animal) and nonparametric (cellular and human studies) analysis as appropriate. $P < 0.05$ was considered statistically significant. The results from animals were expressed as mean ± SE since normal distribution for each data set was confirmed by histogram analyses and Kolmogorov–Smirnov test. In this case, statistical analysis was carried out by parametric analysis. Multiple comparisons were analyzed by two-way analysis of variance followed by Sidak's multiple-comparison test. The results from cellular in vitro mechanistic cell experiments were expressed as mean ± range of *n* experiments. In this case, statistical analysis was carried out by nonparametric analysis. Nonparametric tests were also used to compare the results from human samples of control and IPF patients (Fig. 1 in the main manuscript). In this case, data were displayed as medians, interquartile range, and minimum and maximum values. In both nonparametric analyses, statistical analysis was carried out by Mann–Whitney or Kruskal–Wallis test when comparing two or more groups, respectively.

ACKNOWLEDGEMENTS

This work was supported by the grants Fondo Europeo de Desarrollo Regional (FEDER) and Isntituto de salud carlos III FIS PI17/02158 (J.M.), JR18/00050 (J.M.), SAF2017-82913-R (J.C.), RTI2018-096827-B-I00 (E.M.), CIBERES (CB06/06/0027), and TRACE (TRA2009-0311), of the Spanish Government, and by research grants from the Regional Government Prometeo 2017/023/UV (J.C., E.M.), ACIF/2016/341 (B.B.) from "Generalitat Valenciana". Funding entities did not contribute to the study design or data collection, analysis and interpretation, or to the writing of the paper.

AUTHOR CONTRIBUTIONS

J.M., B.B., M.J.S., J.E., E.A., E.M., and J.C. designed and performed experiments and data analysis; J.M., B.B., J.E., M.J.S., E.A., E.M., and J.C. designed experiments and oversaw all data analyses; J.M., B.B., E.A., M.J.S., J.E., E.A., E.M., and J.C. drafted the paper. All authors have critically revised the paper. All authors have read, reviewed, and approved the final paper as submitted to take public responsibility for it.

ADDITIONAL INFORMATION

The online version of this article (https://doi.org/10.1038/s41385-020-00343-w) contains supplementary material, which is available to authorized users.

Competing interests: The authors declare no competing interests.

Publisher's note Springer Nature remains neutral with regard to jurisdictional claims in published maps and institutional affiliations.

REFERENCES

1. Wolters, P. J., Collard, H. R. & Jones, K. D. Pathogenesis of idiopathic pulmonary fibrosis. *Annu. Rev. Pathol.* **9**, 157–179 (2014).
2. Bagnato, G. & Harari, S. Cellular interactions in the pathogenesis of interstitial lung diseases. European respiratory review: an official journal of the European Respiratory. *Society* **24**, 102–114 (2015).
3. Selman, M. & Pardo, A. Revealing the pathogenic and aging-related mechanisms of the enigmatic idiopathic pulmonary fibrosis. an integral model. *Am. J. Respir. Crit. Care Med.* **189**, 1161–1172 (2014).
4. Richeldi, L. et al. Efficacy and safety of nintedanib in idiopathic pulmonary fibrosis. *N. Engl. J. Med.* **370**, 2071–2082 (2014).
5. King, T. E. Jr. et al. A phase 3 trial of pirfenidone in patients with idiopathic pulmonary fibrosis. *N. Engl. J. Med.* **370**, 2083–2092 (2014).
6. Lederer, D. J. & Martinez, F. J. Idiopathic pulmonary fibrosis. *N. Engl. J. Med.* **378**, 1811–1823 (2018).
7. Ballester, B., Milara, J. & Cortijo, J. Mucins as a new frontier in pulmonary fibrosis. *J. Clin. Med.* **8**, 1447 (2019).
8. Seibold, M. A. et al. A common MUC5B promoter polymorphism and pulmonary fibrosis. *N. Engl. J. Med.* **364**, 1503–1512 (2011).
9. Lorenzo-Salazar, J. M. et al. Novel idiopathic pulmonary fibrosis susceptibility variants revealed by deep sequencing. *ERJ Open Res.* **5**, 00071 (2019).
10. Hoffmann, J. et al. Distinct differences in gene expression patterns in pulmonary arteries of patients with chronic obstructive pulmonary disease and idiopathic pulmonary fibrosis with pulmonary hypertension. *Am. J. Respir. Crit. Care Med.* **190**, 98–111 (2014).
11. Mukhopadhyay, P. et al. MUC4 overexpression augments cell migration and metastasis through EGFR family proteins in triple negative breast cancer cells. *PLoS ONE* **8**, e54455 (2013).
12. Wang, G. et al. Detection of the potential pancreatic cancer marker MUC4 in serum using surface-enhanced Raman scattering. *Anal. Chem.* **83**, 2554–2561 (2011).
13. Hattrup, C. L. & Gendler, S. J. Structure and function of the cell surface (tethered) mucins. *Annu. Rev. Physiol.* **70**, 431–457 (2008).
14. Gautam, S. K. et al. MUC4 mucin- a therapeutic target for pancreatic ductal adenocarcinoma. *Expert Opin. Therap targ.* **21**, 657–669 (2017).
15. Zhi, X. et al. MUC4-induced nuclear translocation of beta-catenin: a novel mechanism for growth, metastasis and angiogenesis in pancreatic cancer. *Cancer Lett.* **346**, 104–113 (2014).
16. Ponnusamy, M. P. et al. MUC4 activates HER2 signalling and enhances the motility of human ovarian cancer cells. *Br. J. Cancer* **99**, 520–526 (2008).
17. Rachagani, S. et al. MUC4 potentiates invasion and metastasis of pancreatic cancer cells through stabilization of fibroblast growth factor receptor 1. *Carcinogenesis* **33**, 1953–1964 (2012).
18. Jonckheere, N. et al. The mucin MUC4 and its membrane partner ErbB2 regulate biological properties of human CAPAN-2 pancreatic cancer cells via different signalling pathways. *PLoS ONE* **7**, e32232 (2012).
19. Fernandez, I. E. & Eickelberg, O. The impact of TGF-beta on lung fibrosis: from targeting to biomarkers. *Proc. Am. Thorac. Soc.* **9**, 111–116 (2012).
20. Morris, D. G. et al. Loss of integrin alpha(v)beta6-mediated TGF-beta activation causes Mmp12-dependent emphysema. *Nature* **422**, 169–173 (2003).
21. Munger, J. S. et al. The integrin alpha v beta 6 binds and activates latent TGF beta 1: a mechanism for regulating pulmonary inflammation and fibrosis. *Cell* **96**, 319–328 (1999).
22. Milara, J. et al. MUC4 impairs the anti-inflammatory effects of corticosteroids in patients with chronic rhinosinusitis with nasal polyps. *J. Allerg. Clin. Immunol.* **139**, 855–862 e813 (2017).
23. Reynolds, I. S. et al. Mucin glycoproteins block apoptosis; promote invasion, proliferation, and migration; and cause chemoresistance through diverse pathways in epithelial cancers. *Cancer Metastasis Rev.* **38**, 237–257 (2019).
24. Shorr, A. F., Wainright, J. L., Cors, C. S., Lettieri, C. J. & Nathan, S. D. Pulmonary hypertension in patients with pulmonary fibrosis awaiting lung transplant. *Eur. Respir. J.* **30**, 715–721 (2007).
25. Yokoyama, S. et al. Aberrant methylation of MUC1 and MUC4 promoters are potential prognostic biomarkers for pancreatic ductal adenocarcinomas. *Oncotarget* **7**, 42553–42565 (2016).

26. Nakano, Y. et al. MUC5B promoter variant rs35705950 affects MUC5B expression in the distal airways in idiopathic pulmonary fibrosis. *Am. J. Respir. Crit. Care Med.* **193**, 464–466 (2016).
27. van Putten, J. P. M. & Strijbis, K. Transmembrane mucins: signaling receptors at the intersection of inflammation and cancer. *J. Innate Immun.* **9**, 281–299 (2017).
28. Funes, M., Miller, J. K., Lai, C., Carraway, K. L. 3rd & Sweeney, C. The mucin Muc4 potentiates neuregulin signaling by increasing the cell-surface populations of ErbB2 and ErbB3. *J. Biol. Chem.* **281**, 19310–19319 (2006).
29. Theodoropoulos, G., Carraway, C. A. & Carraway, K. L. MUC4 involvement in ErbB2/ErbB3 phosphorylation and signaling in response to airway cell mechanical injury. *J. Cell. Biochem.* **107**, 112–122 (2009).
30. Ponnusamy, M. P. et al. Emerging role of mucins in epithelial to mesenchymal transition. *Curr. Cancer Drug Targets* **13**, 945–956 (2013).
31. Epstein Shochet, G., Brook, E., Eyal, O., Edelstein, E. & Shitrit, D. Epidermal growth factor receptor paracrine upregulation in idiopathic pulmonary fibrosis fibroblasts is blocked by nintedanib. *Am. J. Physiol. Lung Cell. Mol. Physiol.* **316**, L1025–L1034 (2019).
32. Vallath, S., Hynds, R. E., Succony, L., Janes, S. M. & Giangreco, A. Targeting EGFR signalling in chronic lung disease: therapeutic challenges and opportunities. *Eur. Respir. J.* **44**, 513–522 (2014).
33. Workman, H. C., Sweeney, C. & Carraway, K. L. 3rd The membrane mucin Muc4 inhibits apoptosis induced by multiple insults via ErbB2-dependent and ErbB2-independent mechanisms. *Cancer Res.* **69**, 2845–2852 (2009).
34. Mora, A. L., Rojas, M., Pardo, A. & Selman, M. Emerging therapies for idiopathic pulmonary fibrosis, a progressive age-related disease. *Nat. Rev. Drug Discov.* **16**, 810 (2017).
35. Kramann, R., DiRocco, D. P. & Humphreys, B. D. Understanding the origin, activation and regulation of matrix-producing myofibroblasts for treatment of fibrotic disease. *J. Pathol.* **231**, 273–289 (2013).
36. Akhurst, R. J. & Hata, A. Targeting the TGFbeta signalling pathway in disease. *Nat. Rev. Drug Discov.* **11**, 790–811 (2012).
37. Milara, J. et al. JAK2 mediates lung fibrosis, pulmonary vascular remodelling and hypertension in idiopathic pulmonary fibrosis: an experimental study. *Thorax* **73**, 519–529 (2018).
38. Chapman, H. A. et al. Reversal of TGFbeta1-driven profibrotic state in patients with pulmonary fibrosis. *N. Engl. J. Med.* **382**, 1068–1070 (2020).
39. Gorina, E. et al. Lung fibrosis measured by quantitative high resolution computed tomography (qHRCT) in idiopathic pulmonary fibrosis (IPF) patients treated with pamrevlumab (FG-3019). *Am. J. Respir. Crit. Care Med.* **197**, A7688 (2018).
40. Murray, L. A. et al. Targeting interleukin-13 with tralokinumab attenuates lung fibrosis and epithelial damage in a humanized SCID idiopathic pulmonary fibrosis model. *Am. J. Respir. Cell Mol. Biol.* **50**, 985–994 (2014).
41. Hecker, L. et al. Reversal of persistent fibrosis in aging by targeting Nox4-Nrf2 redox imbalance. *Sci. Transl. Med.* **6**, 231ra247 (2014).
42. Wang, T., Liu, Y., Zou, J. F. & Cheng, Z. S. Interleukin-17 induces human alveolar epithelial to mesenchymal cell transition via the TGF-beta1 mediated Smad2/3 and ERK1/2 activation. *PLoS ONE* **12**, e0183972 (2017).
43. Epstein Shochet, G., Brook, E., Bardenstein-Wald, B. & Shitrit, D. TGF-beta pathway activation by idiopathic pulmonary fibrosis (IPF) fibroblast derived soluble factors is mediated by IL-6 trans-signaling. *Respir. Res.* **21**, 56 (2020).
44. Lehmann, M. et al. Senolytic drugs target alveolar epithelial cell function and attenuate experimental lung fibrosis ex vivo. *Eur. Respir. J.* **50**, 2 (2017).
45. Raghu, G. et al. An official ATS/ERS/JRS/ALAT clinical practice guideline: treatment of idiopathic pulmonary fibrosis. an update of the 2011 clinical practice guideline. *Am. J. Respir. Crit. Care Med.* **192**, e3–e19 (2015).
46. Milara, J. et al. Aclidinium inhibits human lung fibroblast to myofibroblast transition. *Thorax* **67**, 229–237 (2012).
47. Milara, J. et al. The JAK2 pathway is activated in idiopathic pulmonary fibrosis. *Respir. Res.* **19**, 24 (2018).
48. Almudever, P. et al. Role of tetrahydrobiopterin in pulmonary vascular remodelling associated with pulmonary fibrosis. *Thorax* **68**, 938–948 (2013).
49. Kilkenny, C., Browne, W. J., Cuthill, I. C., Emerson, M. & Altman, D. G. Improving bioscience research reporting: the ARRIVE guidelines for reporting animal research. *Plos Biol.* **8**, e1000412 (2010).